Precision Clinical Medicine, 2(4), 2019, 221–234

doi: 10.1093/pcmedi/pbz028
Advance Access Publication Date: 8 December 2019
Research Article

RESEARCH ARTICLE

DNA methylome study of human cerebellar tissues identified genes and pathways possibly involved in essential tremor

Jennifer L. Paul[1], Khashayar Dashtipour[2], Zhong Chen[1] and Charles Wang[1,3*]

[1]Center for Genomics, School of Medicine, Loma Linda University, Loma Linda, CA 92350, USA; [2]Division of Movement Disorders, Department of Neurology, Loma Linda University Medical Center, Loma Linda, CA 92350, USA; [3]Department of Basic Sciences, School of Medicine, Loma Linda University, Loma Linda, CA 92350, USA

*Correspondence: Charles Wang, chwang@llu.edu

Abstract

Background: Essential tremor (ET) is a neurological syndrome of unknown origin with poorly understood etiology and pathogenesis. It is suggested that the cerebellum and its tracts may be involved in the pathophysiology of ET. DNA methylome interrogation of cerebellar tissue may help shine some light on the understanding of the mechanism of the development of ET. Our study used postmortem human cerebellum tissue samples collected from 12 ET patients and 11 matched non-ET controls for DNA methylome study to identify differentially methylated genes in ET.

Results: Using Nugen's Ovation reduced representation bisulfite sequencing (RRBS), we identified 753 genes encompassing 938 CpG sites with significant differences in DNA methylation between the ET and the control group. Identified genes were further analyzed with Ingenuity Pathway Analysis (IPA) by which we identified certain significant pathways, upstream regulators, diseases and functions, and networks associated with ET.

Conclusions: Our study provides evidence that there are significant differences in DNA methylation patterns between the ET and control samples, suggesting that the methylation alteration of certain genes in the cerebellum may be associated with ET pathogenesis. The identified genes allude to the GABAergic hypothesis which supports the notation that ET is a neurodegenerative disease, particularly involving the cerebellum.

Key words: DNA methylome; reduced representation bisulfite sequencing; essential tremor; cerebellum; epigenetics; CpGs

Background

Essential tremor (ET) is a neurological syndrome of unknown origin, resulting in bilateral upper-limb action tremors[1]. As this prolongs for a minimum of 3 years, it may be accompanied by tremors in other locations but without neurological signs[1]. If neurological signs are indeed present and lacking clinical significance, it

Received: 18 October 2019; **Revised:** 30 November 2019; **Accepted:** 1 December 2019

Table 1. Demographics of essential tremor and control participants.

Demographics	Essential Tremor (N = 12)	Control (N = 11)	*P*-value
Expired age, years (Mean ± SD)	83.3 ± 3.8	84.9± 4.9	>0.05
Female (%)	41.7	45.5	
Male (%)	58.3	54.5	
Brain weight, grams (Mean ± SD)	1197.8 ± 156.3	1166.4 ± 54.3	>0.05
Last MMSE* test score (Mean ± SD)	28.5 ± 1.8	27.8 ± 1.2	>0.05

Demographic information for both ET and control groups are displayed. The Folstein Mini Mental State Examination score is a game performance score measuring cognitive function. The average age at expiration, gender, brain weight and last MMSE test score were not significantly different between the two groups.
MMSE, Folstein Mini Mental State Examination score; SD: standard deviation. *the Folstein Mini Mental State Examination score is a game performance score measuring cognitive function.

is criteria for classification as essential tremor plus[1]. ET may initiate asymptomatically and the tremors may be mild, however as time progresses the symptoms worsen at an estimated 2%-5% per year[2]. It primarily affects adults, although it may occur at any age. Risk factors include older age and family history[3]. ET remains one of the most common movement disorders[4] affecting 1% of the population[5]. Yet, the etiology and pathogenesis of ET remains poorly understood. The diagnosis relies on clinical assessments, as there is no valid biomarker to detect it. Generally, neurologic examinations and comprehensive medical history are utilized in assessment to rule out other known causes. Due to the nature of ET's unknown origin and the lacking of biomarkers, the clinical diagnosis contributes to only moderately effective therapies and pharmacological treatments.

Our study utilizes human cerebellum tissues for DNA methylome analysis, offering insight into changes undergone in the cerebellum of ET patients. The cerebellum is becoming a primary interest in ET research as it is suggested that the cerebellum and its tracts may be involved in the pathophysiology for ET[4]. Growing evidence exists for a unique role of the cerebellum in ET, including clinical[6,7], neuroimaging[8–11], neurochemical and pathological studies[12]. Clinical studies have documented cerebellar signs in ET[13,14], including cerebellar vermis atrophy[10]. Additionally, controlled postmortem studies have documented changes in the cerebellar cortex in ET, specifically with a loss of Purkinje cells[15,16].

Epigenetics refers to DNA modifications that affect gene activity but do not change the DNA sequence. Epigenetic change has been involved in neurological disease pathogenesis[17]. It was also found that the epigenetic reprogramming is involved in brain development, neuronal differentiation and cognition[18]. Investigation of epigenetic alterations, particularly the differential DNA methylation in the cerebellum, may lead to a better understanding of the mechanism for the development of ET. Identifying epigenetic changes in ET may offer insight into potential predispositions, gene-environment interactions, and therapeutic agents. Currently, there is no report that investigates the DNA methylome using cerebellum tissues from ET patients. However, DNA methylome alterations have been documented in other neurodegenerative disorders[19]. Environmental factors can alter phenotype through epigenetics, which can be heritable through cell division and a transgenerational fashion[20]. Yet, DNA methylation presents itself as an ideal target mechanism to focus on because epigenetic changes are essentially reversible[21]. Additionally, it will be beneficial to explore the biological pathways involved in the genes associated with epigenetic changes.

This study aims to identify DNA methylation patterns in the cerebellar tissues of ET patients. We performed genome-wide DNA methylation by reduced representation bisulfite sequencing (RRBS) aimed to examine differentially methylated CpG sites/genes and conducted pathway analysis based on the differentially methylated genes. We identified 938 CpG sites belonging to 753 genes, with significant differences in methylation between ET patients and controls.

Results

Sample demographics

Our study included the data collected from 12 samples in the ET group and 11 samples in the control group. Patient demographics for each postmortem cerebellar tissue sample harvested for DNA processing are summarized in Table 1. The ET participants were on average ~83 years of age at expiration and ~58% male. The average brain weight was ~1,198 grams and the average last Folstein Mini Mental State Examination (MMSE) score was 28.5. Similarly, the controls were on average ~85 years of age at expiration and ~55% male with an average brain weight of ~1,166 grams and last MMSE test score of 27.8. The average age at expiration, gender, brain weight and last MMSE test score were not significantly different between the two groups.

RRBS data quality

High quality reads were obtained from RRBS data (Supplementary Figure 1). We aligned the RRBS methylome data, 70 bp single reads, to the NCBI human GRCh38 genome. On average, 63.4% of the reads were aligned to the genome. The aligned reads were further annotated, resulting in 1.06 million overlapped CpG sites (the CpG

A

Context	Methylated	SD	Methylation (%)
CpG	5,221,512	338,552	44.15
CHG	162,060	11,940	1.11
CHH	464,949	35,797	1.35

B

Context	Methylated	SD	Methylation (%)
CpG	5,261,707	218,658	43.90
CHG	161,589	17,975	1.08
CHH	462,606	63,967	1.33

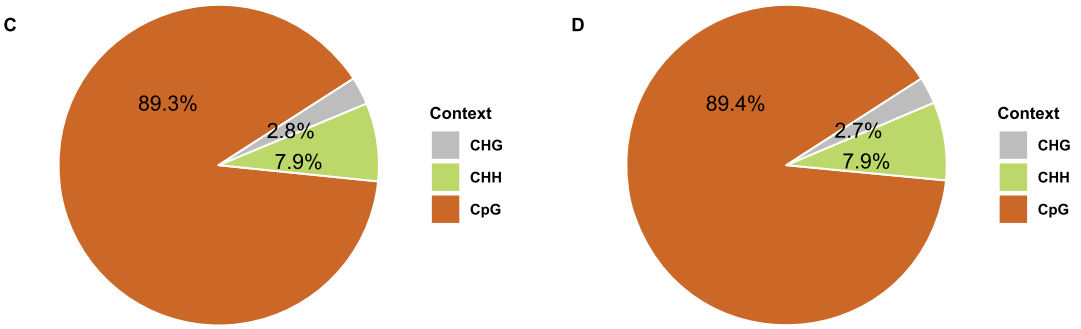

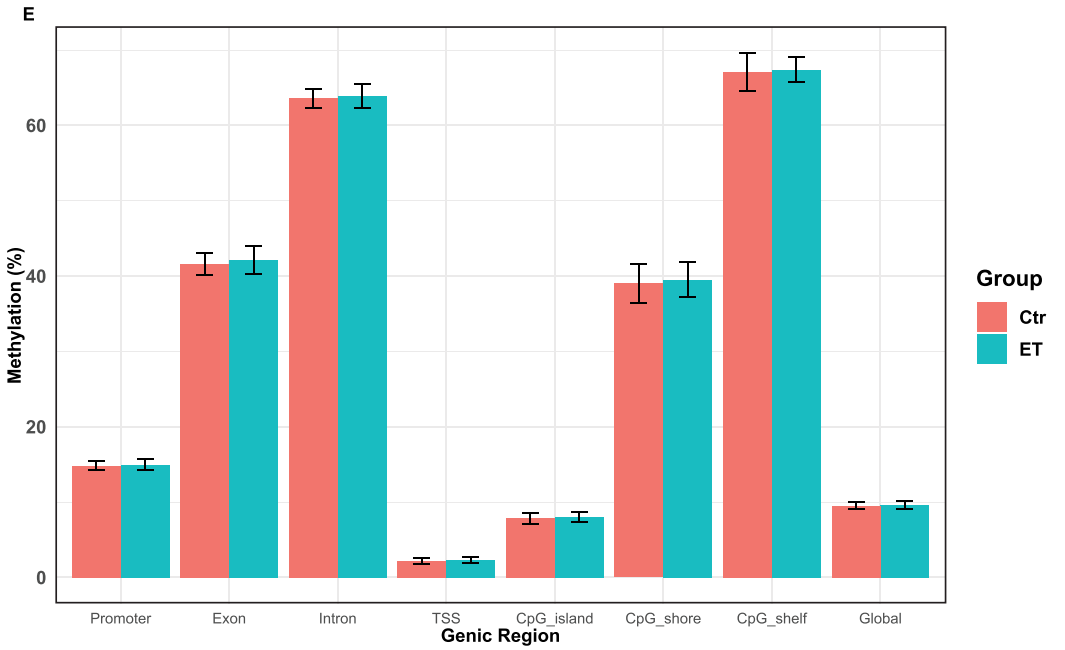

Figure 1. Characterization of genome-wide DNA methylation in cerebellum tissues. The proportion of methylation at each context to the total methylation detected was presented for the control group **(A)** and ET group **(B).** The average methylation status of cytosine at CpG, CHG and CHH contexts across all samples for the control group **(C)** and the ET group **(D); (E)** methylation of CpG at genic regions between ET and control are presented. Data was the average and standard deviation of all CpG annotated to each genic region from all samples of each group. SD: standard deviation.

site was present in at least 9 samples in each group) covered by at least 10 reads.

Genome-wide methylation

An average of 5.8 million methylated cytosine residues per sample were detected from our RRBS dataset. No difference in global methylation or the distribution of the methylated cytosine in DNA context was observed between control and ET groups (Fig. 1A and B). The genome-wide cytosine methylation rate in the CpG context was about 44%, which was significantly higher than those in the CHG and CHH contexts (1.1%, and 1.3%, respectively) (Fig. 1A and B). Out of those methylated cytosine residues, over 89% were in the CpG context, 7.9% were in the CHH context and less than 3% were in the CHG context (Fig. 1C and D). We further examined the CpG methylation at genic region. Data revealed that the transcription start site (TSS) had the lowest methylation rate, followed by the CpG islands and the

promoter region. Overall, CpG methylation in these three regions was much lower than the global CpG methylation ($p < 0.001$, Fig. 1E). The methylation rate at exon and CpG shore regions was similar to global CpG methylation; while intron and CpG shelf region exhibited much higher methylation than the rest of the genic regions. Our genome-wide methylation data is consistent with other human methylome studies. We observed a consistent small increase in CpG methylation at the TSS, exon and CpG shore regions in the ET group, but the differences were not significant ($p = 0.156$ for TSS, $p = 0.196$ for exon, $p = 0.321$ for CpG shore) (Fig. 1E). Our data suggested that there were methylation changes in the ET cerebellum samples.

Methylation of CpG islands

All together 753 genes with differentially methylated CpG sites (DMCs) that were present in at least 9 samples (80% of the group) were identified with a 15% difference in methylation ($p < 0.05$). A total of 938 DMCs with a minimum of 15% difference in methylation ($p < 0.05$) were detected between the ET and control group. The DMCs were located mainly in intergenic (41%) and intron (35%) regions, followed by 14% in the exon and 10% in the promoter regions (Fig. 2A and B). Among the DMCs, 58.1% were hypomethylated and 41.9% were hypermethylated (Fig. 2C), which showed similar distributions across the gene body. All genes categorized into gene families with 5 or more DMCs combined are summarized in Supplementary File 1. The complete analysis can be found in Supplementary File 2. These gene families included: zinc finger protein, long intergenic non-protein coding RNA, microRNA, rho GTPase activating protein, solute carrier family, collagen type, protocadherin, UDP glucuronosyltransferase, ankyrin, pleckstrin homology domain containing, ring finger protein, family with sequence similarity, nuclear receptor, transmembrane protein, ATPase, coiled-coil domain containing, hook microtubule tethering protein, mitogen-activated protein kinase, zinc finger and BTB domain containing, huntingtin interacting protein, member RAS oncogene, and tripartite motif containing. Three gene families (UDP glucuronosyltransferase, mitogen-activated protein kinase, huntingtin interacting protein) had same trends in methylation patterns. In the UDP glucuronosyltransferase and huntingtin interacting protein genes, every DMC was hypermethylated. In mitogen-activated protein kinase genes, each DMC was hypomethylated. The largest family of genes identified, composed of 17 individual genes and 27 total DMCs, was the zinc finger protein family. Data suggested these genes were tightly regulated at epigenetic level. Statistical analysis confirmed that methylation change in ET patients was not a random event (Supplementary File 2).

We found that there was no significant difference in methylation around the TSS region [-200 bp to +200 bp,

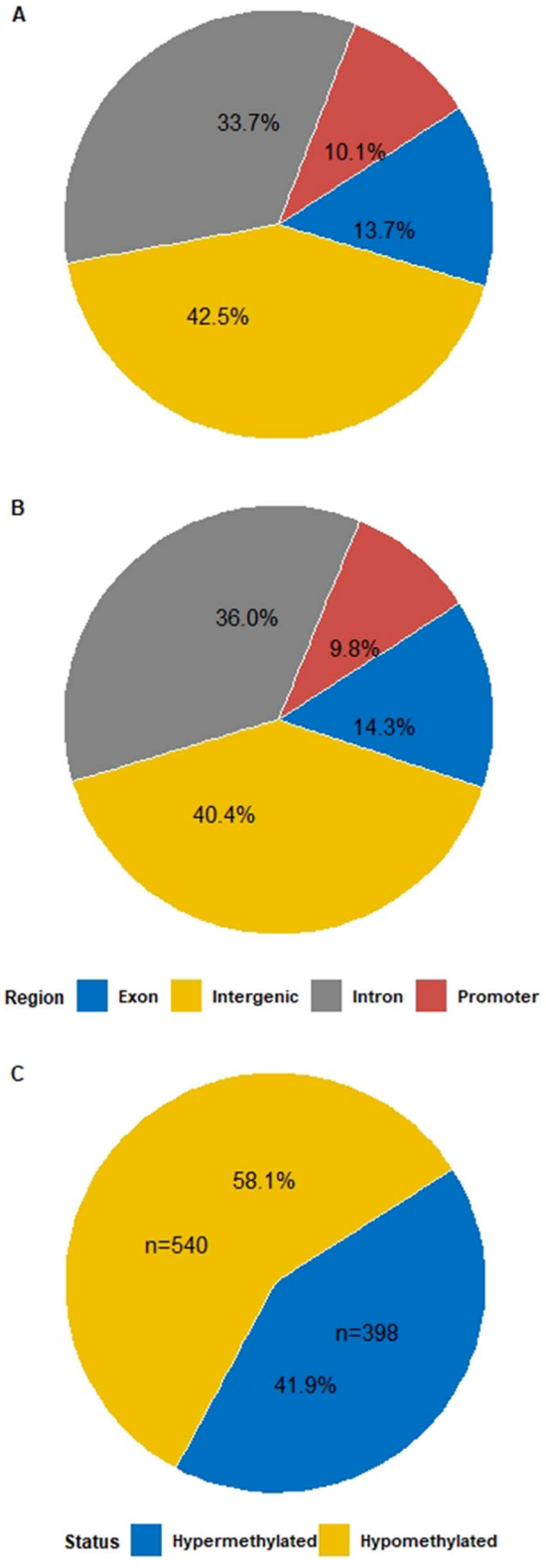

Figure 2. Differentially methylated CpGs (DMCs) in cerebellum between ET and control. Location distribution of hypermethylated DMCs **(A)** and hypomethylated DMCs **(B)** in genes by intergenic, intron, exon, and promoter region **(C)** Methylation status by percentage of hyper- and hypomethylated CpGs.

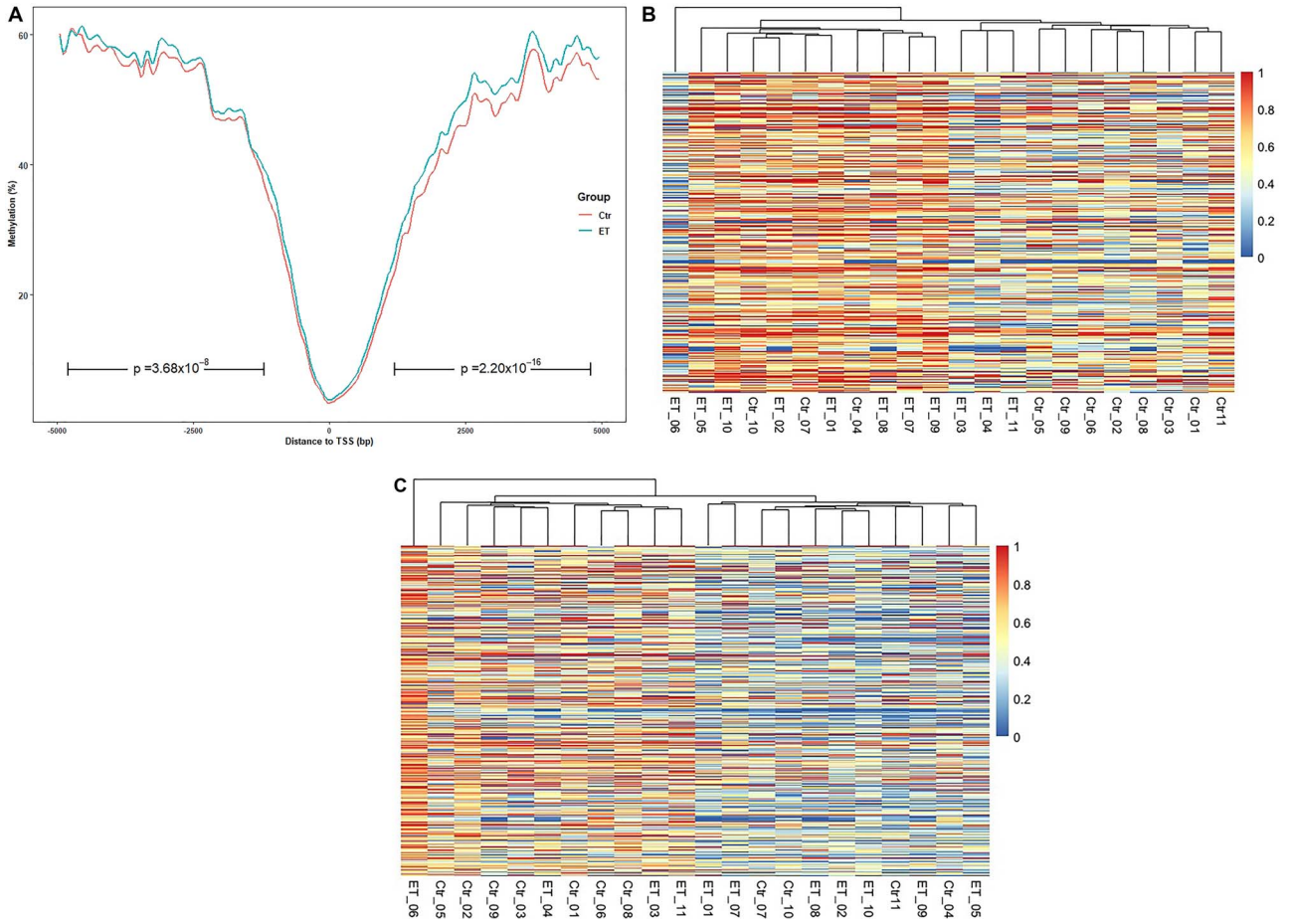

Figure 3. Visualization of methylation difference between ET and control. (A) Methylation level of CpGs flanking to TSS. All CpGs annotated within 5 kb of TSS were included. The region from ≥ 1 kb upstream and region from ≤ -1 kb downstream are significantly different. N = 12 in ET group and N = 11 in control group. Heat map of hypermethylated CpG **(B)** and hypomethylated CpG. **(C)** loci. Only CpGs that are annotated to known genes were selected for the heat map plot. Due to space limitation, the CpG information is not shown on the plot, but listed in Supplementary File 3. Hierarchical cluster analysis on sample dissimilarity was calculated using the "complete" method.

the CpGs flanking the TSS], but the difference was significant at regions beyond 1 kb from the TSS (Figure 3A). The methylation at 1 kb or greater downstream from the TSS, mostly within the gene body, was significantly higher in the ET group compared to the control group ($p = 3.68 \times 10^{-8}$). Similarly, the methylation at 1 kb or greater upstream from the TSS was also significantly higher in the ET group as compared to the control group ($p = 2.20 \times 10^{-16}$). Our results also showed that ET patients had significant methylation difference at either gene regulatory region (promoter and enhancers) and/or gene body at global genic level (Fig. 3A).

In order to display the methylation difference between ET and control samples, DMCs annotated to known genes were selected for hierarchical cluster (heat map) plotting. Methylation beta values of 492 hypermethylated loci and 370 hypomethylated loci were presented (Fig. 3B and C, respectively). Hierarchical clustering uncovered differences in methylation at group level across all CpG loci. (Each row represents a CpG locus. CpG information was not shown on the heat map due to limitation in space but can be found in Supplementary File 3). Given that the CpGs present in at least 9 samples in each group were merged for DMC analysis, the heterogeneity shown in the heat map may indicate variation in the RRBS dataset. Nevertheless, the majority of ET samples showed consistent higher methylation in hypermethylated loci and lower methylation in hypomethylated loci compared to the control.

To find out if there was a differential methylation (DM) within a gene body on the top hypermethylated and hypomethylated genes between ET and control, we examined methylation profiles for the top 5 genes with the highest number of significant hypermethylated CpGs (ZNF664, HOOK2, PTPRN2, CCDC92, and COL18A1) as well as the top 5 genes with the highest number of significant hypomethylated CpGs (ARHGAP27P1, ZFYVE28, ARHGAP45, ARHGEF10L and COL5A1). Nevertheless, for these 10 genes, there was no difference in the methylation of specific gene parts between ET and control (Fig. 4).

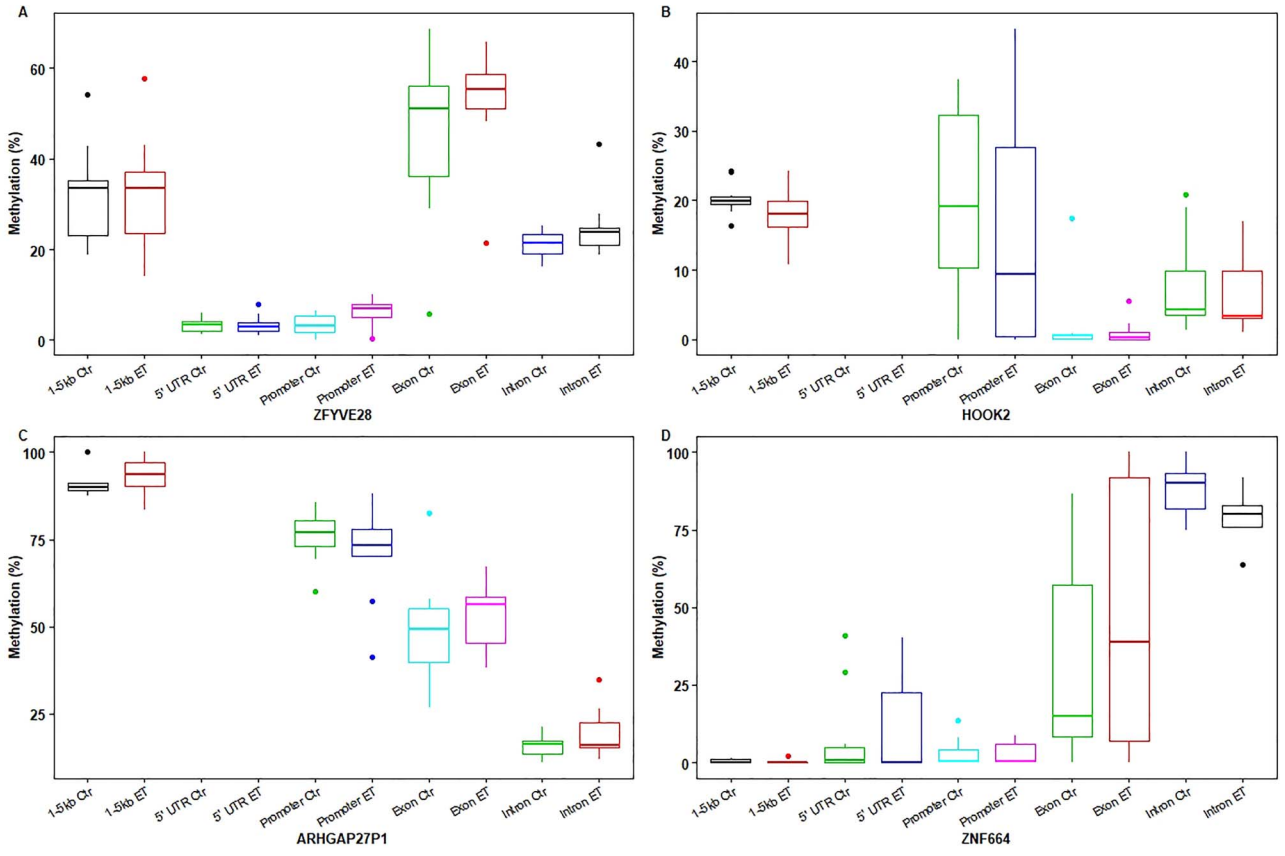

Figure 4. Methylation level across different regions within gene body. CpG methylation levels in relation to gene body for (**A**) ZFYVE28, (**B**) HOOK2, (**C**) ARHGAP27P1 and (**D**) ZNF664. There was no difference between ET and control groups in the methylation percentage of specific gene parts of these tested genes.

Table 2. Top canonical pathways associated with selected top differentially methylated genes.

Canonical pathways	P-value	Overlap ratio (%)
GP6 signaling pathway	1.24E-04	6/118 (0.051)
Hepatic fibrosis/hepatic stellate cell activation	9.32E-04	6/172 (0.035)
Calcium transport I	1.48E-03	2/9 (0.222)
Thyroid hormone metabolism II (via conjugation and/or degradation)	7.48E-03	2/20 (0.100)
Apelin liver signaling pathway	1.16E-02	2/25 (0.080)

Canonical pathway analysis identifies the pathways from the IPA library that are most significantly enriched in the selected differentially methylated genes from the Supplementary File 1 with differentially methylated CpG sites. IPA measures significance of association via Fisher's exact test with a P-value and the overlap ratio, the ratio of the number of genes identified/presented in our significant DMGs that map to the pathway divided by the total number of genes in that pathway in IPA.

IPA on significant differentially methylated genes

We ran the selected differentially methylated genes (DMGs) through Ingenuity Pathway Analysis (IPA). Our IPA identified 11 significant canonical pathways as being significantly enriched with these genes. The pathways included GP6 signaling pathway, hepatic fibrosis/hepatic, stellate cell activation, calcium transport I, thyroid hormone metabolism II (via conjugation and/or degradation), apelin liver signaling pathway, nicotine degradation III, melatonin degradation I, nicotine degradation II, superpathway of melatonin degradation, apelin cardiomyocyte signaling pathway, and serotonin degradation. The top 5 most significant pathways are described in Table 2 with *P* value and overlap ratio. While comparing the GP6 signaling pathway against the hepatic fibrosis/hepatic stellate cell activation pathway, we identified the following genes as commonly presented in both: COL18A1, COL23A1, COL27A1, COL4A2, COL5A1, and COL6A3. ATP2B2 and ATP2B4 were identified in the calcium transport I pathway, while UGT1A1 and UGTA6 were identified in the thyroid hormone metabolism II. COL18A1 and MAPL12 were identified in the apelin liver signaling pathway.

There were 13 upstream regulators identified by IPA (Table 3). Of these regulators, 9 were translation regulators: AGO2, RAD21, CTCF, NFKB1, PITX3, RELA,

Table 3. Upstream regulators on the expression of significant molecules and genes.

Upstream Regulators	Molecule Type	P-value	Target Molecules
AGO2	Translation regulator	9.16E-04	MIR-136, MIR-219, MIR-431, MIR-433
let-7	microRNA	2.18E-03	COL27A1, NR2E1
RAD21	Transcription regulator	4.66E-03	PCDHGA4, PCDHGB1
CLN3	Other	6.45E-03	HOOK1
TTN	Kinase	6.45E-03	ANKRD2
CTCF	Transcription regulator	7.26E-03	PCDHGA4, PCDHGB1
TNFSF12	Cytokine	8.75E-03	ANKRD2, MIR-133
NFKB1	Transcription regulator	1.04E-02	ANKRD2, NR4A3
PITX3	Transcription regulator	1.29E-02	MIR-133
RELA	Transcription regulator	1.30E-02	ANKRD2, NR4A3
MYOD1	Transcription regulator	1.92E-02	ANKRD2
MKNK1	Kinase	2.29E-02	FAM49A, MAPK8IP3, NR4A3
FOS	Transcription regulator	3.55E-02	ANKRD2, COL18A1
NOTCH3	Transcription regulator	4.43E-02	COL5A1

IPA identified any molecule as an upstream regulator if it can regulate the expression of other molecules in the dataset including transcription factors, miRNA, drugs, compounds, etc. P-value of overlap was calculated by IPA using Fisher's exact test to determine overlap between genes in the data set to genes known in the literature to be regulated by upstream regulators.

Table 4. Top Diseases and bio-functions identified by IPA.

Diseases and bio functions		P-value range	Number of Molecules
Disease and Disorders	Auditory Disease	1.31E-02 - 4.19E-04	2
	Neurological Disease	4.25E-02 - 4.19E-04	11
	Organismal Injury and Abnormalities	2.60E-02 - 4.19E-04	8
	Infectious Diseases	3.23E-02 - 6.55E-03	1
	Immunological Disease	9.26E-03 - 9.26E-03	3
Molecular and Cellular Functions	Cell Morphology	1.31E-02 - 4.19E-04	2
	DNA Replication, Recombination, and Repair	4.80E-03 - 4.80E-03	2
	Cell-To-Cell Signaling and Interaction	4.50E-02 - 6.55E-03	3
	Cellular Assembly and Organization	6.55E-03 - 6.55E-03	1
	Cellular Function and Maintenance	1.95E-02 - 6.55E-03	2
Physiological System Development and Function	Auditory and Vestibular System Development and Function	1.95E-02 - 4.19E-04	2
	Nervous System Development and Function	4.50E-02 - 4.19E-04	10
	Organ Morphology	4.50E-02 - 4.19E-04	6
	Organismal Development	4.50E-02 - 4.19E-04	6

IPA identified the known diseases and biological functions that our dataset molecules were associated with. The numbers of molecules associated are listed with each disease or function. IPA calculates p-value by the right tail Fisher exact test.

MYOD1, FOS, and NOTCH3. There were 2 kinases, TTN and MKNK1. In addition, Let-7, a microRNA, CLN3, under the "other" category, and TNFSF12, a cytokine, were also identified as one of the upstream regulators.

Top disease and disorders were auditory disease, neurological disease, organismal injury and abnormalities, infectious diseases, and immunological disease. Top molecular and cellular functions were cell morphology, DNA replication, recombination, and repair, cell-to-cell signaling interaction, cellular assembly and organization, and cellular function and maintenance. Top physiological system development and functions included auditory and vestibular system development and function, nervous system development and function, organ morphology, organismal development and tissue morphology. The top diseases and biological functions are summarized in Table 4.

Significant IPA networks were also identified based on our significant DMGs that are highly interconnected (Fig. 5). Each network was described with the top 3 diseases and functions associated, as well as a network score based on the number of the DMGs in the network. Network 1, with a score of 24, was Nervous System Development and Function, Organ Morphology, and Organismal Development. This first network centers on beta-estradiol, amyloid beta precursor protein (APP), and huntingtin (HTT). APP was associated with the MAPL8IP3, RNF213, FAM49A and ATP2B2 genes in the significant DMG dataset as portrayed in the network. According to Ingenuity Expert Findings, mutations of the MAPL8IP3 gene in the brains of mice exhibiting Alzheimer's disease increases expression of a product of the APP protein. HTT is also closely associated with some molecules in our dataset. Mutant HIP1 genes have been shown in mice to

Path Designer Network 1

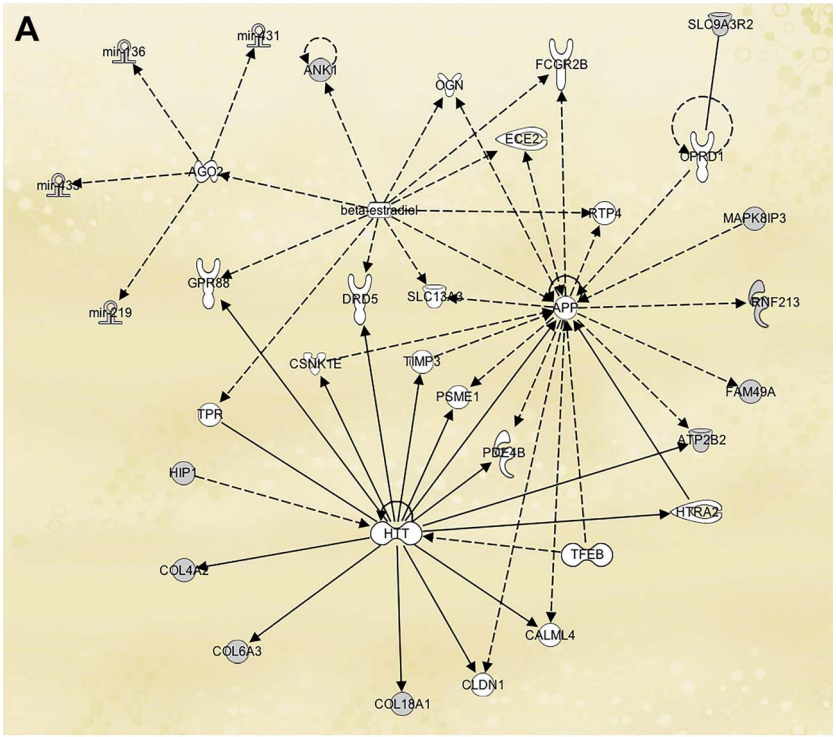

Path Designer Network 2

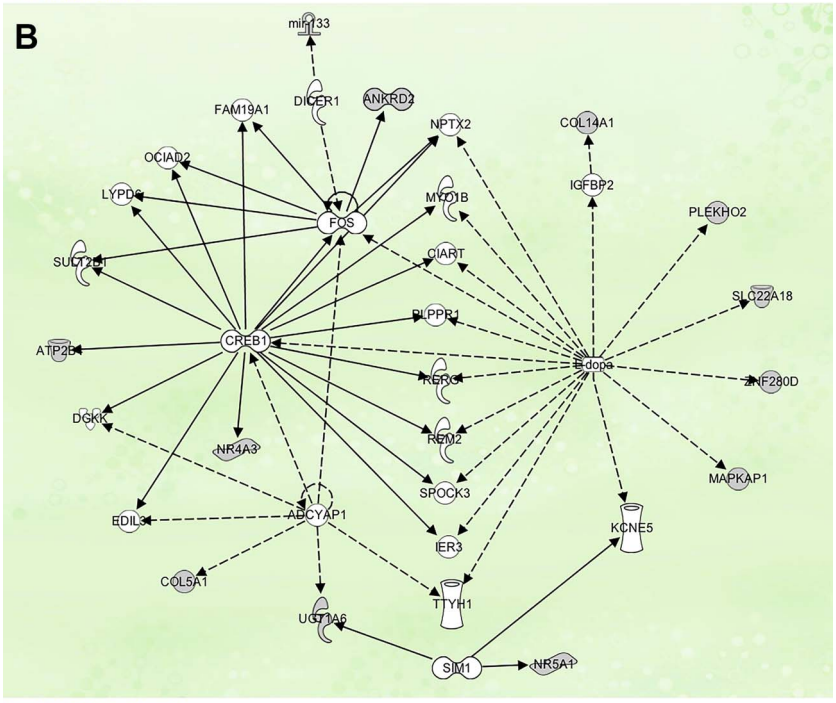

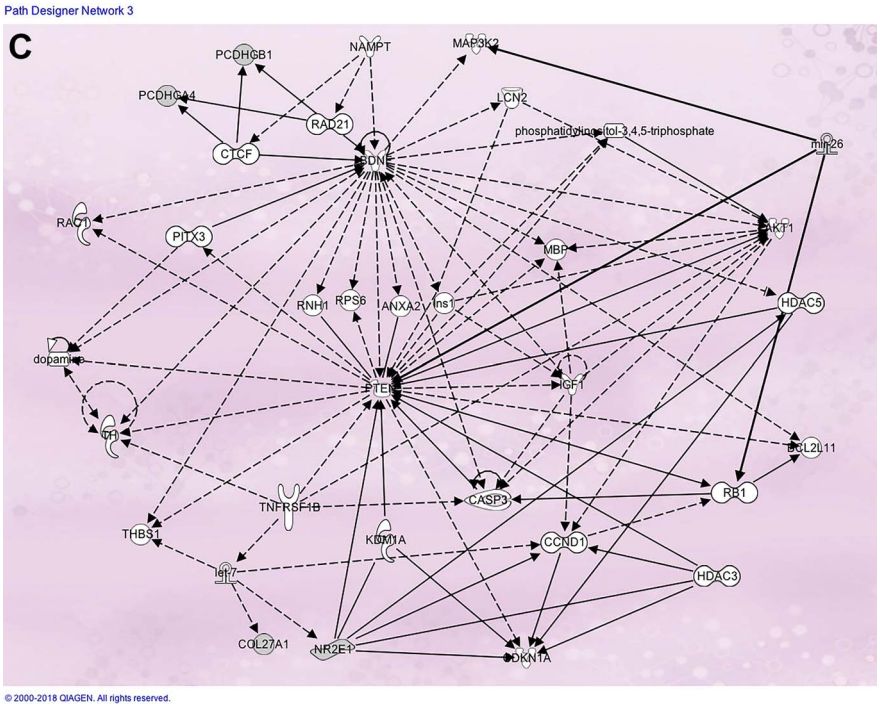

Figure 5. The top three significant networks identified by IPA. Each network had 35 molecules that were identified by IPA as highly interconnected. The network score was based on the number of dataset molecules in the network and the negative log value of Fisher's Exact test. **(A)** Network 1 with a network score of 24. The top three diseases and functions associated with this network were Nervous System Development and Function, Organ Morphology, and Organismal Development. **(B)** Network 2 with a network score of 20. The top three diseases and functions associated with this network were Cell Death and Survival, Cancer, and Neurological Disease. **(C)** Network 3 with a network score of 6. The top three diseases and functions associated with this network were Embryonic Development, Endocrine System Development and Function, and Nervous System Development and Function.

increase phosphorylation of the HTT protein in cortical neurons and decrease expression of COL18A1 mRNA, COL4A2 mRNA, and COL6A3 mRNA in differentiating neurons. Network 2, with a score of 20, was Cell Death and Survival, Cancer, and Neurological Disease. The network's primary molecules were fos proto-oncogene (FOS), cAMP responsive element binding protein 1 (CREB1), L-dopa, and adenylate cyclase activating polypeptide 1 (ADCYAP1). Some of the significant DMGs that were significantly associated with this network include ANKRD2, NR4A3, ATP2B4, COL5A1, and UGT1A6. In mice, the FOS protein is involved in the activation of a DNA endogenous promoter from the ANKRD2 gene in diaphragm muscle. In T98G human glioblastoma cells, interference of CREB1 mRNA decreases expression of NR4A3 mRNA and there is binding between the CREB1 protein and DNA endogenous promoter from NR4A3 gene. The CREB1 protein decreases expression of ATP2B4 mRNA in mouse hippocampal neurons and the ADCYAP1 protein increases expression of COL5A1 and UGT1A6 mRNA in mouse pituitary gland. Network 3, with a score of 6, was Embryonic Development, Endocrine System Development and Function, and Nervous System Development and Function. The key molecules in this network were brain derived neurotrophic factor (BDNF) and phosphate and tensin homolog. BDNF is linked to the significant DMGs RAD21 and CTFT through protein-DNA interactions. Both the RAD21 and CTFT human proteins have been shown to bind with DNA endogenous promoters containing a conserved sequence element from the human PCDHGB1 and PCDHGA4 genes in neuroblastoma cell line SK-N-SH cells. The NR2E1 protein is associated with binding to and increasing expression of PTEN mRNA in neural stem cells from mouse brain. Human PTEN mRNA is targeted by MIR26A mature microRNAs in LN229 glioblastoma multiforme cells.

Discussion

We were able to identify many genes that may be associated with ET and have been shown in the literature to be involved in the pathogenesis of neurological diseases. Zinc-finger proteins (ZNFs) possess the ability to interact with DNA, RNA, PAR and other proteins. ZNF alterations are involved in the development of several diseases including neurodegeneration[22]. Other zinc finger proteins not identified in this study have previously been linked to the cerebellum. Mutant ZNK423 with deleted functional domains leads to premature cell

cycle exit, Purkinje cell progenitor pool deletion, and impaired Purkinje cell differentiation[23]. ZFP423 mutation also leads to a loss of the corpus callosum, reduction of the hippocampus and malformation of the cerebellum such as agenesis of the vermis[24]. Another family with 4 genes as identified in our significant DMG list between ET and control, rho GTPase activating protein, was found together to have 22 CpGs. Rho GTPases are involved in neurodevelopment and also play a role in central nervous system diseases including intellectual disability, autism spectrum disorder, Alzheimer's disease and Schizophrenia[25]. Rho proteins have also been directly linked to Purkinje cell death. In organotypic cultures of mice, an inhibitor of GTPase Rho increased survival of Purkinje cells[26]. Protocadherin genes, which are cell-cell adhesion molecules that typically have high expression in the nervous system, were identified as one of most significant DMGs as well. Previous research has linked epigenetic dysregulation of protocadherins to disease pathogenesis as other studies apart from ours have also found alterations in DNA methylation in postmortem brains of patients with brain disorders[27]. Additionally, mutations or epigenetic dysregulation in reprogramming machinery have been linked to many neurodevelopmental and neurodegenerative disorders[27]. *ANK1* gene functions in muscle and brain cells in cell stability and cell movement[28]. Early alterations in brain DNA methylation of this gene have been associated with Alzheimer's disease pathology[29]. Furthermore, in *ANK 1* deficient mice in which Purkinje and granule cells were depleted of *ANK1*, there was Purkinje cell loss and neurological symptoms[30]. Disease-associated ANK1 CpG site hypermethylation in the entorhinal cortex was found in neurological diseases including Alzhiemer's disease, Huntington's disease, and Parkinson's disease. The same study found *ANK1* hypermethylation at 5 CpG sites in the cerebellum in Alzheimer's disease[31]. Several ATPase genes were identified in our study. Defects in Na^+, K^+-ATPase in the brain have been linked to neuronal hyper excitability and epilepsy, and activity is lower in the brains of Alzheimer's disease patients[32]. Huntingtin interacting proteins, known to have lost their function of interaction with the huntingtin protein in Huntington's disease[33], were found to be hypermethylated in our study. Members of RAS oncogene family are associated with neurodevelopmental disorder with ataxic gait and decreased cortical white matter[34]. Tripartite motif containing was found to have altered expression in Alzheimer's disease brains[35]. Overall, our study has identified a large number of significant DMCs which are distributed in many different gene families that have been associated with other neurological diseases in the past.

Based on the significant DMCs and DMGs, IP A was able to provide significant upstream regulators, and associated networks, pathways and diseases and functions. Many of the upstream regulators had cellular components and subcellular locations that included neurites and neuron projections, perikaryons, and nerve endings and synapses. TTN has cellular components and subcellular locations pertaining to muscle anatomy such as the A band, I band, M band, Z disc, muscle myosin complex, myofibril, sarcomere, and striated muscle thin filament. Based on the ingenuity knowledge base, we found that many of these upstream regulators are associated with various neurological diseases and movement disorders such as Alzheimer's disease, Parkinson's disease, multiple sclerosis, schizophrenia, Cornelia de Lange syndrome, neuronal ceroid lipofuscinosis, seizures/epileptic seizures, resting tremor, fetal akinesia, gait disturbances, Huntington's disease, familial amyloidotic polyneuropathy, and kindling, suggesting the common important epigenetic regulation involved in these neurological disorders. According to Gene Ontology (GO) annotations, six of these regulators are involved in biological processes involving development, cell differentiation, muscle contractions and other processes. The development processes are related to the nervous system, forebrain, midbrain, and neurons, while the cell differentiation is related to dopaminergic neuron differentiation, negative regulation of neuron differentiation, and positive regulation of Schwann cell differentiation. Meanwhile, TTN is a regulator associated with muscle contraction, actin cytoskeleton organization, and muscle filament sliding. Lastly, other processes probably playing a role in ET include the negative regulation of neuron apoptotic process, neuromuscular process controlling balance, neurotransmitter metabolic process, negative regulation of gliogenesis, negative regulation of neurogenesis, and positive regulation of neuron apoptotic process.

Our gene network analysis indicated that the top IPA category in diseases and disorders that had the most molecules was "neurological" and the top category for physiological system development and function was "nervous system". Most of the functions from these two categories overlapped. Briefly, many functions included abnormal morphology, size and quantity, and development, formation, and generation. Abnormal morphology included that of the dilated fourth cerebral ventricle, auditory cortex, diencephalon, parietal lobe, vestibulocochlear nerve, outer hair cells, and dorsal telencephalic commissure, as well as morphogenesis of the anterior commissure and telencephalon. Development, formation, and generation pertained to the development of radial glial palisade, ventromedial nucleus of hypothalamus and of commissure. It is clear that many significant DMGs in our ET study are involved in the brain and its functions.

Significant networks were discovered to be associated with the DMGs. The first network centers on beta-estradiol, amyloid beta precursor protein (APP), and

huntingtin (HTT), all molecules that are associated with diseases such as Alzheimer's, Parkinson's or Huntington's disease. While none of our patients had been diagnosed with Alzheimer's, Parkinson's or Huntington's disease, one element that links those diseases and molecules together is neurodegeneration. APP and HTT are linked to neurodegeneration, tremor, memory deficits, cognitive impairment, dementia, ataxia and depression. The second network's primary molecules were FOS, cAMP responsive element binding protein 1 (CREB1), L-dopa, and adenylate cyclase activating polypeptide 1 (ADCYAP1). L-dopa is a drug used for the reduction of tremors and motor symptoms in Parkinson's disease. CREB1 is associated with neurodegeneration as well, while FOS is associated with motor dysfunction and seizures. The third significant network's key molecules were brain derived neurotrophic factor (BDNF) and phosphate and tensin homolog (PTEN). Of particular importance, BDNF and PTEN are both associated with the GABAergic biological process. BDNF is also linked to Huntington's disease, Alzheimer's and Parkinson's disease, amyotrophic lateral sclerosis, Rett syndrome, neurodegeneration, depression, anxiety, motor dysfunction, ataxia, tremor and seizures. These networks allude to possible disease etiology hypotheses that are already postulated in the literature. Of particular interest are neurodegeneration and the GABAergic system. There is some debate as to whether ET is a neurodegenerative disease[36], but experts in the field point to the neurodegeneration hypothesis and the GABAergic hypothesis as two of the major etiology hypotheses due to a wealth of supporting data[37]. In the network 3 of IPA analysis, molecules BDNF and PTEN are involved in the GABAergic system. Our current study based on DNA methylation indicates that certain DMGs are associated with the GABAergic system, supporting the gamma-aminobutyric acid (GABA) hypothesis for ET. The GABA hypothesis with respect to ET is the idea that there is a disturbance that is decreasing the activity of the GABAergic system, particularly involving the cerebellum[38]. This is one of the most robust pathophysiological hypotheses for ET[38]. More data needs to be collected to confirm if different methylation patterns are influencing the GABA activity in the cerebellum[38].

One drawback of our study is the lack of an evaluation of the methylation effect on gene expression due to the fact that RNA was degraded in the human cerebellum samples archived. We suggest that future studies include gene expression, such as RNA-seq, to allow an integration analysis of methylome and transcriptome. We note that there was no significant difference in DNA methylation in a few previously reported ET candidate genes such as LINGO 1, TREM2, or SLC1A2.

Conclusion

Our DNA methylome study using DNA extracted from cerebellar tissues from both ET patients and controls identified 753 DMGs comprising 938 DMCs which are primarily in the intergenic and intron regions. Based on the DMGs identified, our gene network and IPA analyses suggest the biological plausibility of many DMGs and the IPA regulators, diseases, functions and networks associated with diseases of similar neurological disorders to ET and conditions of clinical manifestations of ET. Our study is unique in that it investigated the DNA methylation patterns of rarely available human cerebellum tissues from ET patients. Our results suggest that the methylation status of genes in the cerebellum may be associated with ET pathogenesis. Future studies investigating possible therapeutical approaches that enhance the GABA transmission in the cerebellum area may be beneficial[38]. Gene-environment interactions that alter the DNA methylation of the identified genes may provide an avenue for reduced ET by minimizing environmental triggers. Additionally, future research may lead to therapeutic options that target causative epigenetic alterations.

Methods

Patient samples and subject collection

Postmortem human cerebellum tissue samples were used for DNA extraction. Samples were collected from 12 ET patients and 11 matched non-ET controls. These archived tissue samples were obtained from the Banner Sun Health Research Institute's Brain and Body Donation Program. No IRB was needed.

DNA extraction from cerebellum tissues

Dissected cerebellum (~20 mg) was homogenized with Precellys CKM beads in 200 µL of lysis buffer using Qiagen All Prep DNA/RNA/miRNA Universal kit. DNA was extracted following the manufacturer's protocol. DNA quality was analyzed by Agilent's Tapestation 2200 and DNA quantity was determined by Qubit 3.0.

RRBS library construction

Isolated genomics DNA (100 ng) of isolated genomics DNA was used for RRBS library construction using the Ovation® RRBS Methyl-Seq System (NuGEN Technologies, San Carlos, CA) according to the manufacturer's protocol. Briefly, the methylation insensitive MspI enzyme, which cuts the DNA at 5'CCGG3' sites, was used to digest genomics DNA into fragments. The fragments were directly subject to end repair and phosphorylation in preparation for ligation to a methylated adapter with a single-base T overhang. A unique index was used per sample for multiplexing. The ligation products were used for bisulfite conversion using Qiagen EpiTect Fast DNA Bisulfite Kit according to Qiagen's protocol. Bisulfite-converted DNA was then amplified using Mastercycler® pro (Eppendorf, Hamburg, Germany) and bead-purified with Agencourt AMPure Beads. Library concentration was measured by Qubit 3.0 and library

size was determined using Agilent Tapestation 2200 with D1000 screen tape.

RRBS library sequencing and data analysis

Libraries with different barcodes were pooled. Clusters were generated on cBot with HiSeq3000/4000 SR cluster kit from 5 µL of 2 nM template (200 pM at cBot loading). 70-bp single read data was obtained using Illumina HiSeq 4000 and SBS reagents at Loma Linda University Center for Genomics. Using RRBS technology, we analyzed DNA methylation patterns of 11 control and 12 ET samples. A dataset of 518 million, 70-bp single-end reads were generated from HiSeq4000, with an average read depth of 22.5 ± 3.7 millions. One sample was removed from downstream data analysis due to lower read depth. Quality of the sequenced reads for each individual sample was assessed using the FastQC program (Supplementary Fig. 1.) (http://www.bioinformatics.babraham.ac.uk/projects/fastqc). Based on the quality, trimming of the sequence from the 3′ end of the reads was performed with Trim Galore v0.4.5 (https://www.bioinformatics.babraham.ac.uk/projects/trim_galore). The additional sequence added by the NuGen diversity adaptors and the reads that do not contain an MspI site signature YGG at the 5' end were removed by NuGen custom scripts, trimRRBSdiversityAdaptCustomers.py (version 1.10, NuGEN). The sequence reads were then aligned against the human reference genome (hg38) using Bismark aligner (v0.16.334, http://www.bioinformatics.babraham.ac.uk/projects/bismark) with default settings. After alignment, the PCR duplicates were removed with NuGen custom scripts NuDup.py (NuGEN). CpG sites with a minimum coverage of 10 reads in at least 9 samples in each group were used for follow-up analysis. DM was analyzed by MethylKit[39] and annotated using R package "annotatr"[40]. The DM CpGs were selected using a false discovery rate (FDR) < 0.05 and methylation percentage change between control and test groups were > 15%.

Ingenuity Pathway Analysis

For further analysis pertaining to canonical pathways, upstream regulators, diseases and biological functions, and networks, the selected significant DMGs within gene families with 5 or more DMCs were analyzed using Ingenuity® Pathway Analysis (IPA) software (QIAGEN Inc.). In the IPA, specific filters were applied to consider only molecules and/or relationships in the nervous system, as well as skeletal muscle to account for motor symptoms. The algorithms developed for use in IPA are described by Kramer[41].

Ethics Approval and Consent to Participate

This is not applicable as the archived tissues were obtained with no patient identification from the Banner Sun Health Research Institute's Brain and Body Donation Program.

Consent for Publication

Not applicable.

Availability of Dataset

Our RRBS fastq files were submitted to GEO (Access number: GSE134426.

Supplementary data

Supplementary data is available in *Precision Clinical Medicine* online at https://doi.org/10.1083/pcmedi/pbz028.

Acknowledgements

This research was partially supported by the Ardmore Institute of Health (grant No. 2150141, CW), the National Institutes of Health (grant No. S10OD019960 for CW), and Dr. Charles A. Sims' gifts to Loma Linda University (LLU) Center for Genomics. The LLU Center for Genomics is partially supported by the National Institutes of Health (grant No. S10OD019960) and Ardmore Institute of Health (grant No. 2150141) and Charles A. Sims' gift. This study was partially funded by an internal seed grant (LLU Grants for Collaborative and Translational Research grant) awarded to CW and KD. We would also like to thank the following programs which allowed us to obtain human brain tissues for DNA methylome study including: the Banner Sun Health Research Institute's Brain and Body Donation Program (BBDP), which was supported by the National Institute of Neurological Disorders and Stroke (U24 NS072026 National Brain and Tissue Resource for Parkinson's Disease and Related Disorders); the National Institute on Aging (P30 AG19610 Arizona Alzheimer's Disease Core Center); the Arizona Department of Health Services (contract 211002, Arizona Alzheimer's Research Center); the Arizona Biomedical Research Commission (contracts 4001, 0011, 05-901 and 1001 to the Arizona Parkinson's Disease Consortium) and the Michael J. Fox Foundation for Parkinson's Research.

All authors expressed deep sorrow for the passing away of Ms. Stephanie Tashiro who was doing volunteer work helping with acquiring archived brain tissues during the early stage of the project. We would like to dedicate this publication to Ms. Stephanie Tashiro.

Conflict of interest

The authors declare that there is no conflict of interests.

References

1. Bhatia KP, Bain P, Bajaj N, *et al*. Consensus Statement on the classification of tremors. From the task force on tremor of

the International Parkinson and Movement Disorder Society. *Mov Disord* 2018;**33**:75-87. doi: 10.1002/mds.27121.
2. Louis ED, Agnew A, Gillman A, *et al*. Estimating annual rate of decline: prospective, longitudinal data on arm tremor severity in two groups of essential tremor cases. *J Neurol Neurosurg Psychiatry* 2011;**82**:761-765. doi: 10.1136/jnnp.2010.229740.
3. Louis ED, Hernandez N, Rabinowitz D, *et al*. Predicting age of onset in familial essential tremor: how much does age of onset run in families? *Neuroepidemiology* 2013;**40**:269-73. doi: 10.1159/000345253.
4. Clark LN, Louis ED. Essential tremor. *Handb Clin Neurol* 2018;**147**:229–39. doi: 10.1016/B978-0-444-63233-3.00015-4.
5. Louis ED, Ferreira JJ. How common is the most common adult movement disorder? Update on the worldwide prevalence of essential tremor. *Mov Disord* 2010;**25**:534-41. doi: 10.1002/mds.22838.
6. Singer C, Sanchez-Ramos J, Weiner WJ. Gait abnormality in essential tremor. *Mov Disord* 1994;**9**:193-6. doi: 10.1002/mds.870090212.
7. Bares M, Husarova I, Lungu OV. Essential tremor, the cerebellum, and motor timing: towards integrating them into one complex entity. *Tremor Other Hyperkinet Mov (NY)* 2012;**2**: pii: tre-02-93-653-1.
8. Wills AJ, Jenkins IH, Thompson PD, *et al*. Red nuclear and cerebellar but no olivary activation associated with essential tremor: a positron emission tomographic study. *Ann Neurol* 1994;**36**:636-42. doi: 10.1002/ana.410360413.
9. Pagan FL, Butman JA, Dambrosia JM, *et al*. Evaluation of essential tremor with multi-voxel magnetic resonance spectroscopy. *Neurology* 2003;**60**:1344-7. doi: 10.1212/01.wnl.0000065885.15875.0d.
10. Quattrone A, Cerasa A, Messina D, *et al*. Essential head tremor is associated with cerebellar vermis atrophy: a volumetric and voxel-based morphometry MR imaging study. *AJNR Am J Neuroradiol* 2008;**29**:1692-7. doi: 10.3174/ajnr.A1190.
11. Passamonti L, Cerasa A, Quattrone A. Neuroimaging of essential tremor: what is the evidence for cerebellar involvement? *Tremor Other Hyperkinet Mov (N Y)* 2012;**2**. doi: 10.7916/D8F76B8G.
12. Filip P, Lungu OV, Manto MU, Bares M. Linking essential tremor to the cerebellum: physiological evidence. *Cerebellum* 2016;**15**:774-80. doi: 10.1007/s12311-015-0740-2.
13. Deuschl G, Wenzelburger R, Loffler K, *et al*. Essential tremor and cerebellar dysfunction clinical and kinematic analysis of intention tremor. *Brain* 2000;**123**:1568-80 doi: 10.1093/brain/123.8.1568.
14. Rao AK, Gillman A, Louis ED. Quantitative gait analysis in essential tremor reveals impairments that are maintained into advanced age. *Gait Posture* 2011;**34**:65-70 doi: 10.1016/j.gaitpost.2011.03.013.
15. Louis ED, Faust PL, Vonsattel JP, *et al*. Neuropathological changes in essential tremor: 33 cases compared with 21 controls. *Brain* 2007;**130**:3297-307. doi: 10.1093/brain/awm266.
16. Babij R, Lee M, Cortes E, *et al*. Purkinje cell axonal anatomy: quantifying morphometric changes in essential tremor versus control brains. *Brain* 2013;**136**:3051-61. doi: 10.1093/brain/awt238.
17. Qureshi IA, Mehler MF. Understanding neurological disease mechanisms in the era of epigenetics. *JAMA Neurol* 2013;**70**:703-10. doi: 10.1001/jamaneurol.2013.1443.
18. Lardenoije R, Iatrou A, Kenis G *et al*. The epigenetics of aging and neurodegeneration. *Prog Neurobiol* 2015;**131**:21–64. doi: 10.1016/j.pneurobio.2015.05.002.
19. Mattson MP. Methylation and acetylation in nervous system development and neurodegenerative disorders. *Ageing Res Rev* 2003;**2**:329-42. doi: 10.1016/s1568-1637(03)00013-8.
20. Handel AE, Ebers GC, Ramagopalan SV. Epigenetics: molecular mechanisms and implications for disease. *Trends Mol Med* 2010;**16**:7-16. doi: 10.1016/j.molmed.2009.11.003.
21. Henikoff S, Matzke MA. Exploring and explaining epigenetic effects. *Trends Genet* 1997;**13**:293-95. doi: 10.1016/s0168-9525(97)01219-5.
22. Cassandri M, Smirnov A, Novelli F, *et al*. Zinc-finger proteins in health and disease. *Cell Death Discov* 2017;**3**:. doi: 10.1038/cddiscovery.2017.71.
23. Casoni F, Croci L, Bosone C, *et al*. *Zfp423/ZNF423* regulates cell cycle progression, the mode of cell division and the DNA-damage response in Purkinje neuron progenitors. *Development* 2017;**144**:3686-97. doi: 10.1242/dev.155077.
24. Alcaraz WA, Gold DA, Raponi E, *et al*. Zfp423 controls proliferation and differentiation of neural precursors in cerebellar vermis formation. *Proc Natl Acad Sci U S A* 2006;**103**:19424-9. doi: 10.1073/pnas.0609184103.
25. Huang GH, Sun ZL, Li HJ, *et al*. Rho GTPase-activating proteins: Regulators of Rho GTPase activity in neuronal development and CNS diseases. *Mol Cell Neurosci* 2017;**80**:18–31. doi: 10.1016/j.mcn.2017.01.007.
26. Julien S, Schnichels S, Teng H, *et al*. Purkinje cell survival in organotypic cultures: implication of Rho and its downstream effector ROCK. *J Neurosci Res*. 2008;**86**:531-6. doi: 10.1002/jnr.21511.
27. El Hajj N, Dittrich M, Haaf T. Epigenetic dysregulation of protocadherins in human disease. *Semin Cell Dev Biol* 2017;**69**:172–82. doi: 10.1016/j.semcdb.2017.07.007.
28. Reference NLoMUGH. ANK1 gene. https://ghr.nlm.nih.gov/gene/ANK1#sourcesforpage (15 March 2019, date last accessed).
29. De Jager PL, Srivastava G, Lunnon K, *et al*. Alzheimer's disease: early alterations in brain DNA methylation at ANK1, BIN1, RHBDF2 and other loci. *Nat Neurosci* 2014;**17**:1156-63. doi: 10.1038/nn.3786.
30. Peters LL, Birkenmeier CS, Bronson RT, *et al*. Purkinje cell degeneration associated with erythroid ankyrin deficiency in nb/nb mice. *J Cell Biol* 1991;**114**:1233-41. doi: 10.1083/jcb.114.6.1233.
31. Smith AR, Smith RG, Burrage J, *et al*. A cross-brain regions study of ANK1 DNA methylation in different neurodegenerative diseases. *Neurobiol Aging* 2019;**74**:70–6. doi: 10.1016/j.neurobiolaging.2018.09.024.
32. de Lores Arnaiz GR, Ordieres MG. Brain Na(+), K(+)-ATPase activity in aging and disease. *Int J Biomed Sci* 2014;**10**:85-102.
33. Reference NLoMUGH. HIP1 gene. https://ghr.nlm.nih.gov/gene/HIP1 (15 March 2019, date last accessed).
34. Lamers IJC, Reijnders MRF, Venselaar H, *et al*. Recurrent De Novo Mutations Disturbing the GTP/GDP Binding Pocket of RAB11B Cause Intellectual Disability and a Distinctive Brain Phenotype. *Am J Hum Genet* 2017;**101**:824-32. doi: 10.1016/j.ajhg.2017.09.015.
35. Yokota T, Mishra M, Akatsu H, *et al*. Brain site-specific gene expression analysis in Alzheimer's disease patients. *Eur J Clin Invest* 2006;**36**:820-30. doi: 10.1111/j.1365-2362.2006.01722.x.

36. Rajput AH, Adler CH, Shill HA, *et al.* Essential tremor is not a neurodegenerative disease. *Neurodegener Dis Manag* 2012;**2**:259-68. doi: 10.2217/nmt.12.23.
37. Helmich RC, Toni I, Deuschl G, *et al.* The pathophysiology of essential tremor and Parkinson's tremor. *Curr Neurol Neurosci Rep* 2013;**13**:378. doi: 10.1007/s11910-013-0378-8.
38. Gironell A. The GABA hypothesis in essential tremor: lights and shadows. *Tremor Other Hyperkinet Mov (N Y)* 2014;**4**:254. doi: 10.7916/D8SF2T9C.
39. Akalin A, Kormaksson M, Li S, *et al.* MethylKit: a comprehensive R package for the analysis of genome-wide DNA methylation profiles. *Genome Biol* 2012;**13**:R87. doi: 10.1186/gb-2012-13-10-r87.
40. Cavalcante RG, Sartor MA. Annotatr: genomic regions in context. *Bioinformatics* 2017;**33**:2381-3. doi: 10.1093/bioinformatics/btx183.
41. Kramer A, Green J, Pollard J Jr, *et al.* Causal analysis approaches in ingenuity pathway analysis. *Bioinformatics* 2014;**30**:523-30. doi: 10.1093/bioinformatics/btt703.